DSLR Imperfections Extraction From Image For Source Detection

Elena Aminova, Ilya Trapeznikov, Andrey Priorov, Vladimir Khryashchev
P.G. Demidov Yaroslavl State University
Yaroslavl, Russia
lena@piclab.ru, trapeznikoff@list.ru, andcat@yandex.ru, v.khryashchev@uniyar.ac.ru

***Abstract*—Digital images frequently contain the objects which are not true for the depicted scene that can completely change the human perception of provided information. This article proposes an approach to search of the digital image forensics caused by distortions and noise of the Digital Single Lens Reflex (DSLR) devices. The tampered object detection algorithms can find these distortions and imperfections despite their size. Therefore it is necessary to reduce influence of these factors in various stages of image processing and forming in the digital devices. The method of determining the reliability of test image forming in the device under consideration based on the pixel non-uniformity of the device that appears at incident light was suggested.**

I. Introduction

The problem of analyzing the noise of DSLR device has practical application in several areas. Standard methods of filtering the noises which appear at different stages of image formation processing is not efficient in several areas of science and technology. Firstly, the enhancement of medical images, for which the noise presence is a critical problem, is often not solved by well-known median filtering. Secondly, it is not effective for images obtained from astronomical systems for the same reasons. Finally, determining the sensor imperfections of the digital device allows identifying this device among others and using it as evidence in forensic examination. In the images under consideration, size of the object often coincides with the smallest size of median filter mask and therefore it can be lost during the median filtering.

A. Image formation in DSLR devices

In all digital devices the general principles and main processing steps are very similar, despite the different component basis. At consecutive stages of this process, different noises and distortions occur due to various factors (external defects, nonideality of hardware components at manufacturing, artifacts of post processing algorithms). A block diagram of digital image formation is presented in Fig. 1.

In this article the following vital questions for our investigation are discussed:

- what types of distortions and noises appear during the digital image formation;
- is there unique features of the DSLR device;
- is it possible to find the initial device in which the image under consideration was formed?

In order to answer for questions mentioned above, let's see into digital image formation and processing scheme in detail.

At the beginning, the light stream passes through the optical systems of the digital device, where it is refracted several times and enters the photosensitive part of the camera (sensors). At this stage, different types of aberration occur because of the structural irregularities of optical surfaces and external objects (dust, villi, specks) which then appear on the final digital image as artifacts of the DSLR optical part [1], [2], [3].

Because of the component cost and constructive features, most digital cameras have only one CCD matrix composed of elements by a certain pattern which is usually a set of red, green and blue (RGB) spectral filters. This mask is previous to the device sensor and is called an array of color filters (CFA) [4], [5], [6], [7].

As a result of using CFA, each pixel in the image has only one color component associated with it. The missing RGB values are calculated based on the values of neighboring pixels by means of an interpolation operation (demosaicing). Despite the fact that each manufacturer uses its own original interpolation methods, i.e. interpolation cores of different sizes and shapes and various interpolation algorithms, all demosaicing methods can be divided into two broad classes. The first class includes well-known methods, such as the nearest-neighbor method, bilinear and bicubic interpolation [8]. The second one is based on usage of not only the inter-channel interpolation, but also in-channel interpolation, for example, boundary interpolation, constant-shade interpolation, second-order gradients, smoothing, interpolation according to homogeneity analysis, template interpolation, vector-based interpolation, Fourier filtering, etc [9].

After the interpolation procedure, a white balance is performed. At this step, unrealistic color flashes are removed. Thus, objects that are perceived by the human visual system as white will be the same in the formed image. At this stage there are preconditions for the development of hot and dead pixels artifacts [10], [11], fixed pattern noises [12], [13], [14], [15] of the device sensors and distortions due to the usage of Bayer patterns.

Realistic perception is achieved through the use of colorimetric interpretation and gamma correction. It should be mentioned that gamma correction is necessary to redistribute the tone information in such a way that allows the human eye to perceive the brightness more accurately [16]. This is primarily

due to the fact that the digital cameras represent brightness in the linear form but the human eye perceives it in the logarithmic one. Then, the process of noise reducing, smoothing and sharpening is performed to prevent the appearance of color artifacts. These processes are the causes of occurrence the structural noise residual after the filtering procedures and the blocking and interpolation artifacts [17], [18]. At the end of the digital imaging process, the formed image is compressed and saved in the device's memory.

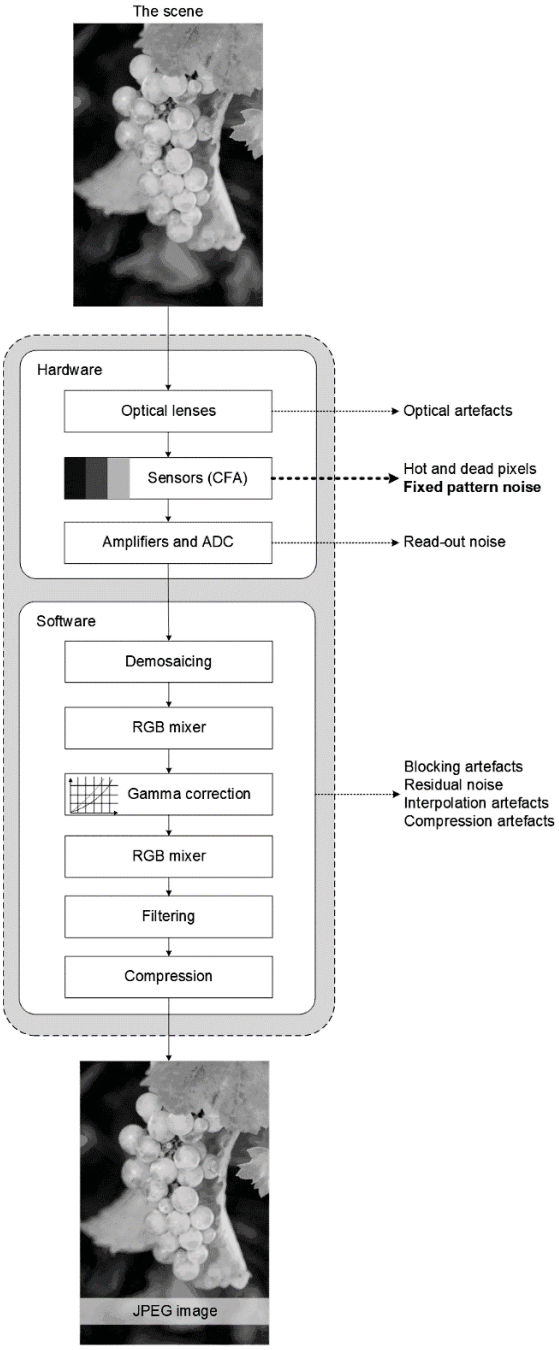

Fig. 1. The main causes for occurrence of the digital device noises and imperfections during digital image formation

It follows from the foregoing that a bunch of irreversible nonlinear operations will be performed at the moment of obtaining the image of the scene. Their order and combination will be unique for each brand, model, device and user settings that can be the basic for distinguishing devices.

B. The causes and types of sensor imperfections

Actually, getting the perfect digital image from digital camera is an unattainable goal. The output digital signal obtained even in case of the uniformly illuminated scene will display small changes in sensitivity between the different pixels. This is partly caused by the shoot noise, also known as photon noise, which is a random process, and structural noise (PN, pattern noise) which is a constant and deterministic noise component [9]. Structural noise is unaltered from image to image of the same scene. Thus structural noise appears on each digital photo taken by the one camera and accordingly can be used later to identify the device. It is properly to call this a systematic distortion rather than a noise. Nevertheless, structural noise is an established term in the technical papers (Fig. 2). It is known that averaging the several images of one scene reduces the random component of the noise and enhances the structural noise.

As already mentioned, the two main components of structural noise are the static structural noise (FPN, fixed pattern noise) and irregular structural noise (PRNU, photo-response non-uniformity). In general, FPN refers to cases when the image sensor is not exposed to the light and is expressed in the difference between intensity of the neighboring pixels. FPN also depends on temperature and illumination.

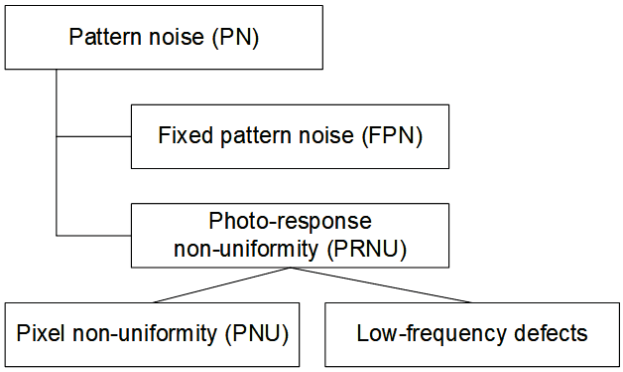

Fig. 2. The main types of sensor pattern noise

In real images, the main part of the structural noise is the non-uniformity of the pixel response (PNU, pixel non-uniformity), which in turn by syne the heterogeneity of the silicon wafers and sensor defects caused during this device manufacturing. Accordingly, it makes this type of noise completely independent of the temperature and humidity of the environment.

Refraction of light on dust particles and reflective surfaces, as well as gain settings makes a significant contribution to PRNU. These components are called low-frequency defects. Because these low-frequency components are not sensor characteristics, they can not be used to identify the camera. Instead of the PNU component is applied for this aim.

The inconspicuous differences between the sensitivity of non-uniformity of the digital device pixel response to the light

flux incident on the photocell cause the PRNU as the CCD (charge-coupled devices) and CMOS (complementary metal-oxide-semiconductor) sensors [4], [5]. PRNU becomes apparent in each obtained from the DSLR device image in the form of a specific unique distribution. Suchwise, it should be possible to answer to the question whether the image was obtained from the considered DSLR device or not.

II. Sensor Imperfections of Digital Devices Detection

C. Premises of sensor imperfections

As mentioned above issue of noise impact on a digital image, it is logical to conclude that some influences result from the very principle of image formation process (e.g. ADC and thermal noise) and are not unique among the technical means. The question of the lens distortions effect in the general case is a separate task and is described in other articles [1, 2, 16]. Therefore, the proposed in this paper approach is based on image formation processing only taking into account the unique causes (influences) that are vital for the mentioned above tasks. As described the aforementioned scheme (Fig. 1), an inefficient pixels and the pre-amplification step (by power supply) of each sensels (a group of sensors), with the followed by ADC operations and quantization of the values gives a matrix of light-signal conversion efficiency coefficients. As is clear from the description, this matrix $\boldsymbol{K}$ equals to the dimension of the sensor matrix of digital device $\boldsymbol{mxn}$. In general, this matrix characterizes PRNU. During the image obtaining process the intensity $\boldsymbol{I}$ of the incident light from the scene gives the response $\boldsymbol{I}+\boldsymbol{IK}$.

The extreme values of $\boldsymbol{K}$ matrix forms hot and dead pixels distributions. It should be mentioned that under normal conditions, the appearance of PRNU impact on the form of $\boldsymbol{K}$ matrix is strongly depended on the intensity of the incident light during the acquisition of the image, according to the $\boldsymbol{IK}$ law. As shown in NASA's research [19], the radiation intensity can be beyond the range of the perceived color range, nevertheless, at the same time activate the sensels.

The described phenomenon known in the science as dark current, manifested in a certain signal level from the sensors at the input of the ADC, even with a closed lens. Continuing to consider hardware about the same level as the dark current has the actual power supply of the sensors. The supply current gives a constant offset $\boldsymbol{O}$ while as the dark current formally depends on the accumulation time and the adjusted sensitivity of the camera and could be expressed as $\boldsymbol{D}$, where $\boldsymbol{D}$ has the dimension of the sensor matrix and $\boldsymbol{mxn}$ and the sense of non-uniformity of the amplifiers and power supply of each element. It is vital to mentioned that any other noises of image processing, which are not previously typified, are accepted as the additive noise $\boldsymbol{N}$.

Output of the sensors in the "raw" format is:

$$Y = I + IK + D + O + N \tag{1}$$

It is well known that in all commercial user devices on hardware level the dark current and offset parameters are corrected automatically. Depending on the selected algorithm for this aims by manufacturers and the user's ISO sensitivity settings, illumination, etc., after implementation of such correction function $\boldsymbol{F}$, the estimation of ε noises, which are unique for each device under consideration at the time of scene fixation, could be calculated as:

$$\varepsilon = F(D + O + N) \tag{2}$$

The final representation of the sensor output taking into account important sensor imperfections:

$$Y = I + IK + \varepsilon \tag{3}$$

The following process $\boldsymbol{P}$ of gamma correction and interpolation are non-linear and dependent on the other pixels of the image operations.

Let go on the per-pixel description for (3):

$$y_{ij} = I_{ij} + I_{ij}K_{ij} + \varepsilon_{ij} \tag{4}$$

where $\boldsymbol{y_{ij}}$ – pixel intensity of the formed digital image, and $\boldsymbol{I_{ij},K_{ij},\varepsilon_{ij}}$ – the intensity of incident light flux, light-signal conversion efficiency coefficient and important sensor imperfections for each pixel $\boldsymbol{ij}$ of the image respectively.

Then the stored pixel values $\boldsymbol{p_{ij}}$ before the compression operation get the following form:

$$p_{ij} = P(y_{ij}, L(y_{ij}), i, j) \tag{5}$$

where $\boldsymbol{L}$ is the local area of neighboring and estimated pixels.

The analysis even in represented (5) form led to considerable difficulties. Thence, let resort to the hypothesis: all non-linear procedures $\boldsymbol{P}$ are considered as a single matrix operator, which influence on the matrix $\boldsymbol{K}$ and is a smaller factor in comparison to hardware defects of digital device.

D. Proposed method of sensor imperfections detection

Based on the description of the output characteristic of the sensor (3), it becomes quite obvious that the original image from the matrix $\boldsymbol{K}$ can be separated by filtering $\boldsymbol{F}$. Assuming the high quality of filtering, whereas allowing the passage of residual noise, it is obtained that:

$$Z = Y - F(Y) = I + IK + \varepsilon - \hat{I} = IK + \theta \tag{6}$$

where is the filtered image, θ is the residual noise.

This approach again requires an image estimation to separate the $\boldsymbol{IK}$ component, which imposes certain constraints on the algorithm $\boldsymbol{A}$. In addition, it is necessary to compensate for the residual noise. All this determines the use of the image database $\boldsymbol{M}$, applying for creating of sensor imperfections pattern of a device under consideration:

$$pattern = \frac{\sum_{n=1}^{M} A_n(Z)}{M} \quad (7)$$

To construct the sensor imperfections structure of a digital device, a set of initial images is used, each of images are applied in the next steps of the distribution formation.

The test image is decomposed into Daubechies wavelets. In the region of obtained transformants, there are special regions (horizontal, vertical, diagonal). The approximate noise level in the Gaussian distribution is determined based on the illumination table. The next step is the scanning of the image with pre-detected areas by the window of 3x3 pixels with subsequent truncation of the noise level values. Similar scanning of the image is also performed using different window sizes to verify the results of the previous step. Then, the regions of interest on the image and high-frequency regions, which are above the noise level, are highlighted. These regions form the stable details of objects in the image. The described steps are carried out for each region of interest in the image. Each special area is divided into a matrix of significant coefficients. As a result, the significant elements of the objects are divided and become equal to the noise level by amplitude. This areas are replaced by the normalized sections. Further, in the region of the Daubechies wavelet transformants, the upper left part of the image is lead to zero. Therefore, the area of transformants contains only residual noise. Then, the inverse wavelet transformation is performed to return from the transform domain to the visible representation. AWGN filter is used to remove the structured areas (depicted objects) of the image. As a result, the pattern of sensor imperfections is obtained. The described process (Fig. 3) is performed for each image formed by the camera under consideration.

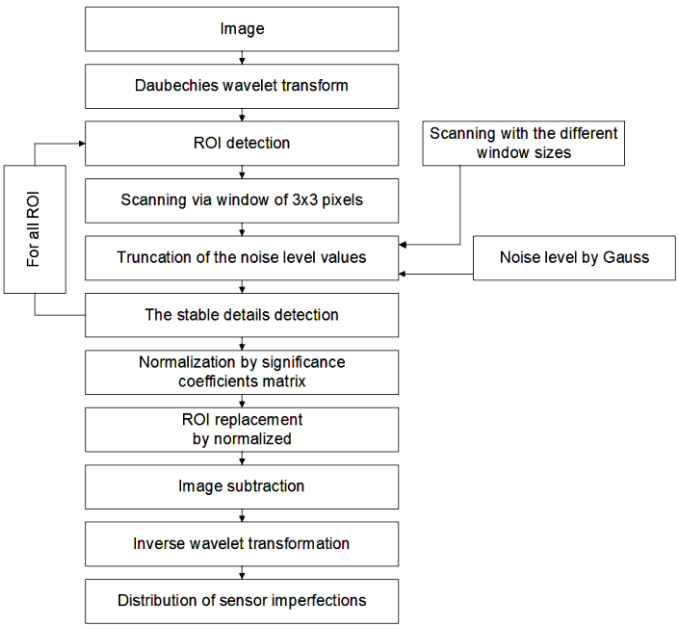

Fig. 3. The proposed algorithm scheme

E. *Detection of image source*

After obtaining the pattern for the selected number of devices, experiments are focused on a search for the maximum of compliance with the hypothesis:

- there is a set of sensor imperfections patterns $patterrn_k$;
- for the test image T, the estimation $A(Z_T) = I_T K + \theta$ is assessed.

Further, cross-correlation among the whole set of the calculated patterns is estimated:

$$p_q = corr(pattern_q, I_T K) \quad (8)$$

The maximum value should be obtained when the test image coincides with the actual device ***T=q***.

The result of verification test image is a correlation field with the presence or absence of a peak value. By the presence, form, significance and severity of the correlation peak, it is possible to conclude that there is a similarity between the two-dimensional distribution of structural noise extracted from the test image was examined and the distribution of the structural imperfections of the proposed DSLR camera. If there is a correlation peak situated in the center against the background of the correlation field values, it is mean that test digital image was formed by the investigated camera. In this case, the thinner the shape of the correlation peak and the greater its value relative to the average energy of the correlation field, the greater the probability that the artifacts of structural imperfections are similar (Fig. 4a). While the image formation by the non-guessed device, the value of the correlation oscillates in the vicinity of zero and the correlation field is homogeneous (Fig. 4b).

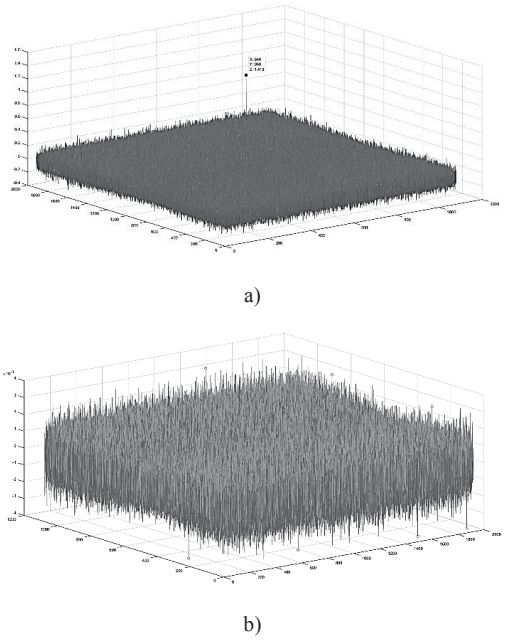

a)

b)

Fig. 4. The results of cross-correlation image classification: a) for true detected image source; b) for false detected image source

III. EXPERIMENTS

A. Image database

To test the suggested method, an original database of test images was created. This database contains 4400 digital images from 44 digital cameras at ones 100 images from each DSLR device. It should be noted that the images have a resolution of at least 1200x600 pixels and have not been modified from the moment of formation to the input of the algorithm. In case that the image has a higher resolution than required value, it was automatically reduced to the demanded size. At the same time, all images were automatically transformed to a horizontal location. The scenes present in the images does not matter, however, the absolutely dark and smooth frames are excluded from the database. Images of the base were obtained both from digital SLR cameras and from cameras of mobile phones. The characteristics of the devices participating for the experiments are presented in Table I. It should be noted that Table I shows the total pixel number.

TABLE I. DSLR DEVICES FOR IMAGE OBTAINING

#	Brand and model	Type of device	Pixels, approx. Mpixels
1	Sony DSLR A700	DSLR camera	12.25
2	Sony DSC W80	DSLR camera	7.2
3	Panasonic DMC-FS5	DSLR camera	10.7
4	Nokia N97	Mobile	5
5	Canon EOS 5D	DSLR camera	12.8
6	Olympus Optical S300D	DSLR camera	3.2
7	Canon EOS 5D Mark II	DSLR camera	21.1
8	Apple Iphone 5s	Mobile	8
9	Pentax k100D Super	DSLR camera	6.31
10	Sony SLT-A37	DSLR camera	16.5
11	Canon EOS 700D	DSLR camera	18.5
12	Canon EOS 40D #1	DSLR camera	10.1
13	Apple Iphone 6	Mobile	8
14	Canon PowerShot A700	DSLR camera	6,2
15	Canon PowerShot A640	DSLR camera	10,3
16	Nokia N95	Mobile	5
17	Olympus SP510UZ	DSLR camera	7.4
18	Canon EOS 40D #2	DSLR camera	10.1
19	Samsung GT-I9000	Mobile	5
20	Apple Iphone 7	Mobile	12
21	Canon EOS 6D #1	DSLR camera	20
22	Canon EOS 6D #2	DSLR camera	20
23	Nikon D5200	DSLR camera	24.7
24-43	Canon EOS 6D #3-#20	DSLR camera	20
44	Nikon D3300	DSLR camera	24.7

B. Sensor imperfections assessment

For the test image of the television optical test table the noise pattern device was constructed. The results of this construction is shown in Fig. 5.

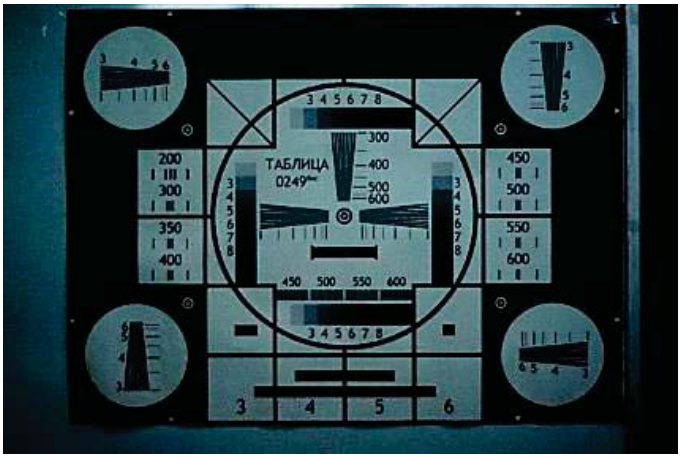

Fig. 5. Example of television optical test table

It is obviously that the constructed distribution, in addition to the clearly noticeable noise component, contains artifacts of the content of the investigated digital image. It should be mentioned that this content is not influence for proposed camera detection algorithm. At the same time, if the digital images from the investigated camera contain the random scene that content artifacts became invisible. The histogram of the noise distribution of camera imperfections artefacts is represented in Fig. 6.

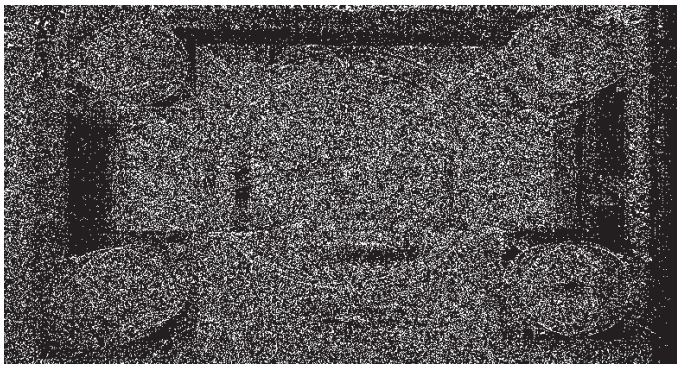

Fig. 6 Camera imperfections artefacts of television optical test table scene

As seen from the constructed histogram, the form of the distribution is close to normal. Consequently, the received noise pattern is characterized by the parameters of the normal distribution (Fig. 7).

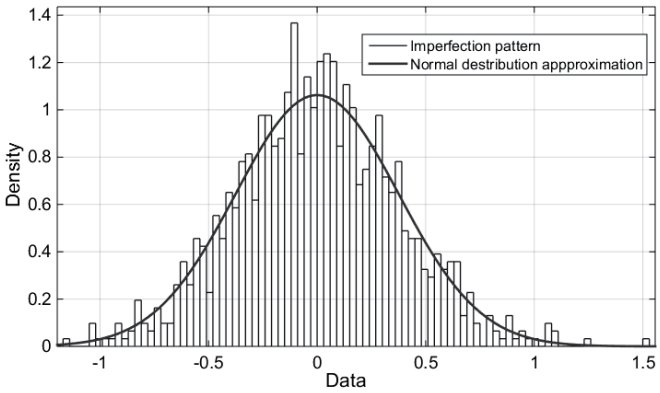

Fig. 7. Device imperfections histogram

To select the essential and sufficient number of images, which is required for the correct operation of the algorithm involved in imperfection pattern construction process, the dependence of the maximum correlation coefficient on the number of images was tested (Fig. 8).

The results underline that the value of peak-correlation energy of the estimate grows almost linearly with increasing number of images. It should be mentioned, the estimated value increases by 2% over the entire range on average. However, the greatest increase in the value of the proposed estimate (by 9%) is observed with the number of used images up to 15.

A test of detection on the device of the test image was carry out from the existing set of 43 different brands and models of devices (Fig. 9).

As can be seen from the graphs, the algorithm made the true decision about whether the test image belongs to the device #21 in case of identification across the entire set of devices.

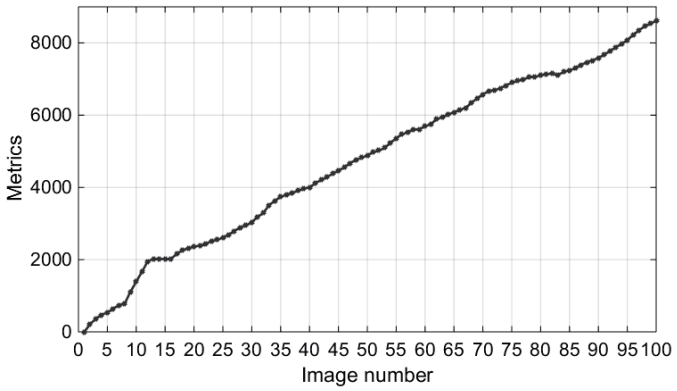

Fig. 8. Peak-correlation-energy in dependence on image number

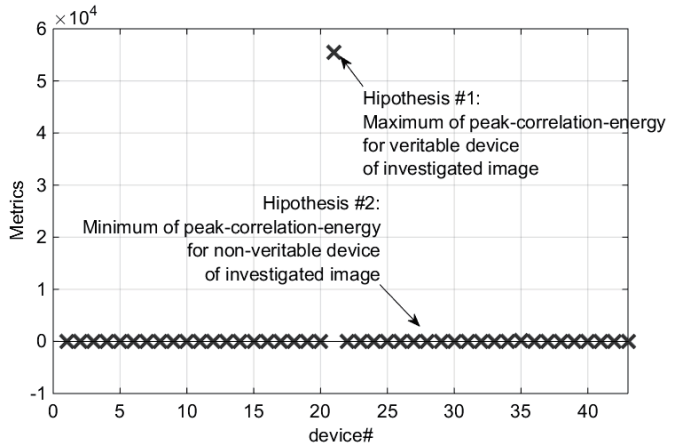

Fig. 9. Camera identification among 43 devices for the test digital image

To evaluate the proposed output criterion of the algorithm – peak-correlation-energy, a comparison of this metrics with well-known correlation approaches: cross-correlation and Pearson correlation was done and performed in Fig. 10.

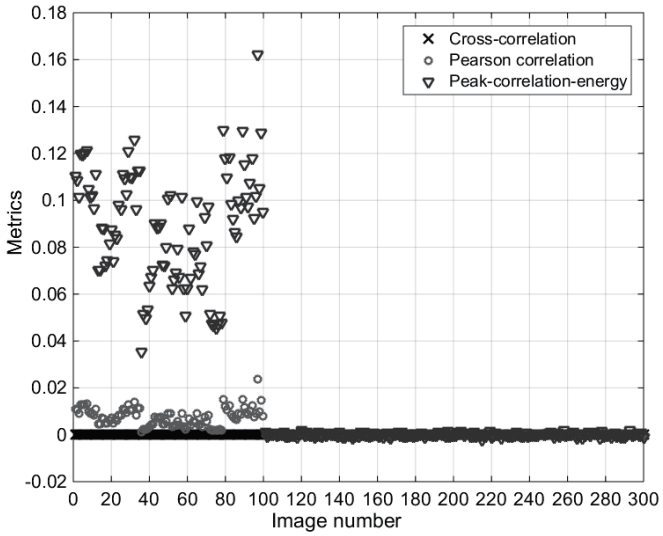

Fig. 10. Comparison of image correlation methods

The test was realized on a set of 300 images by comparing the noise characteristics obtained from these images with the priori known device imperfections feature of Canon 700D. As can be seen from investigation, the proposed method of correlation estimation of images based on the peak-correlation-energy has a large interclass distinguishability of the compared noise patterns for the problem under consideration.

IV. Conclusion

To sum up, presence of the different types of DSLR device distortions and noises is critical for the systems of automatic authentication of digital images. The most significant of them are the sensor imperfections of digital device that arise because of the pixel non-uniformity.

The method considered in this article allows detecting a unique noise distribution of DSLR device sensors and determining device from which the selected image was obtained. In order to test the algorithm the original database of digital images was created in a similar way to [20].

It should be noted that the suggested sensor imperfections distribution is unique characteristic of the DSLR device and can be used for verification of digital images, i.e. for solving the problem of reliability of the digital image obtaining from a particular device under consideration [21].

The peak-correlation-energy is proposed as the output criterion of the algorithm. Testing and analysis of the algorithm are performed based on the original digital image base. Adding images to the set that is used for getting the device imperfections feature increases the metric value by 2% on the average. The number of images in the set should be at least 15 because in this case the greatest increase in the value of the proposed estimate (by 9%) is observed. The proposed estimate of digital image correlation allows to achieve a greater interclass distinctiveness than the Pearson correlation and standard cross-correlation.

ACKNOWLEDGMENT

We would like to thank Yuriy Brjukhanov, Yuriy Lukashevich and Vladimir Volokhov from Yaroslavl State University, who helped us with the equipment to collect database of test images and produced us the opportunity to realize our possibilities. This work was supported by RFBR Grant 15 08-99639-a.

REFERENCES

[1] H. Li and R. Hartley, "A non-iterative method for correcting lens distortion from nine-point correspondences", *In Proc. OmniVision'05, ICCV-workshop,* 2005.

[2] P. R. Gill, C. Lee, D.-G. Lee, A. Wang, and A. Molnar, "A microscale camera using direct fourier-domain scene capture," *Optics Letters*, vol. 36, no. 15, 2011, pp. 2949–2951.

[3] S.-J. Ryu, M. Kirchner, M.-J. Lee, and H.-K. Lee, "Rotation invariant localization of duplicated image regions based on Zernike moments," *IEEE Trans. Inf. Forensics Security*, vol. 8, no. 8, Aug. 2013, pp. 1355–1370.

[4] G.C. Holst, *CCD Arrays, Cameras, and Displays*. 2nd edition, JCD Publishing & SPIE Pres, USA, 1998.

[5] M. Kharrazi, H.T. Sencar, and N. Memon, "Blind Source Camera Identification", *In Proc. ICIP' 04*, Singapore, Oct. 2004, pp. 24–27.

[6] H. Farid and S. Lyu, "Detecting Hidden Messages Using Higher-Order Statistics and Support Vector Machines," *in F.A.P. Petitcolas (ed.): 5th International Workshop on Information Hiding,* LNCS vol. 2578, Springer-Verlag, Berlin-Heidelberg, New York, 2002, pp. 340–354.

[7] J.R. Janesick, "Scientific Charge-Coupled Devices", *SPIE PRESS Monograph, SPIE–The International Society for Optical Engineering*, vol. PM83, 2001.

[8] V. Christlein, C. Riess, J. Jordan, C. Riess, and E. Angelopoulou, "An evaluation of popular copy-move forgery detection approaches", *IEEE Trans. Inf. Forensics Security*, vol. 7, no. 6, , Dec. 2014, pp. 1841–1854.

[9] A. J. Fridrich, B. D. Soukal, and A. J. Lukáš, "Detection of copy-move forgery in digital images," *in Proc. Digit. Forensic Res. Workshop*, 2011.

[10] G.H. Chapman, J. Leung, A. Namburete, I. Koren, and Z. Koren, "Predicting pixel defect rates based on image sensor parameters", *In Proc. IEEE Int. Symposium on Defect and Fault Tolerance*, Vancouver, Canada, Oct. 2011, pp. 408-416.

[11] G.H. Chapman, J. Leung, R. Thomas, I. Koren, and Z. Koren, "Projecting pixel defect rates based on pixel size, sensor area and ISO", *In Proc. Electronic Imaging, Sensors, Cameras, and Systems for Industrial/Scientific Applications XII*, v.8298, 82980E-1-E-11, San Francisco, Jan. 2012.

[12] S. Bayram, H. T. Sencar, and N. Memon, "An efficient and robust method for detecting copy-move forgery," I*n Proc. IEEE Int. Conf. Acoust., Speech Signal Process. (ICASSP)*, Washington, DC, USA, Apr. 2015, pp. 1053–1056.

[13] M. Ghorbani, M. Firouzmand, and A. Faraahi, "DWT-DCT (QCD) based copy-move image forgery detection," *In Proc. 18th Int. Conf. Syst., Signals Image Process. (IWSSIP)*, Jun. 2011, pp. 1–4.

[14] M. Maggioni, E. S. Monge, A. Foi, "Joint removal of random and fixed-pattern noise through spatiotemporal video filtering," I*EEE Trans. Image Processing*, vol. 23(10), Oct. 2014, pp. 4282-4296.

[15] J. E. Pezoa, O. J. Medina, "Spectral model for fixed-pattern-noise in infrared focal-plane arrays," *Progress in Pattern Recognition, Image Analysis, Computer Vision, and Applications – LNCS*, vol. 7042, Nov. 2011, pp. 55-63.

[16] J. Miao, "Coherent diffraction imaging," *Microscopy and Microanalysis*, vol. 20, no. S3, 2014, pp. 368–369,

[17] S. Khan and A. Kulkarni, "Detection of copy-move forgery using multiresolution characteristic of discrete wavelet transform," *In Proc. Int. Conf. Workshop Emerg. Trends Technol. (ICWET)*, New York, NY, USA, 2015, pp. 127–131.

[18] K. Kurosawa, K. Kuroki, and N. Saitoh, "CCD Fingerprint Method - Identification of a Video Camera from Videotaped Images," In Proc. of ICIP'99, Kobe, Japan, Oct. 1999, pp. 537–540.

[19] H.N. Becker, J.W. Alexander, M.D. Dolphin, A.R. Eisenman, P.M. Salomon, L.E. Selva, and D.O. Thorbourn, *Commercial Sensor Survey Fiscal Year 2009 Master Compendium Radiation Test Report*, Jet Propulsion Laboratory California Institute of Technology Pasadena, California, 2010.

[20] M. Goljan, J. Fridrich, and T. Filler, "Large Scale Test of Sensor Fingerprint Camera Identification", *In Proc. SPIE Electronic Imaging, Media Forensics and Security XI*, vol. 7254, San Jose, CA, Jan. 2009, pp. 0I–0J.

[21] E.A. Aminova, I.N. Trapeznikov, and A.L. Priorov, "Overview of digital forensics algorithms in DSLR cameras", *in Proc. Int. Arch. Photogramm. Remote Sens. Spatial Inf. Sci.*, May 2017, pp. 199-205.